CHAPTER I

INTRODUCTION TO THERMOTROPIC LIQUID CRYSTALS

1.0 **Thermotropic** liquid crystals:

The first observation of the liquid crystalline behaviour was made by Reinitzer [1] in the year 1888. He discovered that when cholesteryl benzoate was subjected to the action of heat, it melted at 145°C into a cloudy translucent liquid, which on further heating cleared into a transparent liquid at 178°C. This intermediate cloudy phase existing between the two melting points exhibited some characteristics of both the crystalline solid as well as the isotropic liquid. This new phase was named as liquid crystalline phase and the compounds exhibiting such an intermediate phase or mesophase by the action of heat were called Thermotropic liquid crystals. **A** mesophase that exists above the melting point is called an enantiotropic phase and that which exists below the melting point is called a monotropic phase. Thermotropic liquid crystals are broadly classified into Nematic, Smectic, and Cholesteric liquid crystals based on the orientational and positional ordering of the molecules. In the following section we describe the structure of different types of liquid crystalline phases that are discussed in this thesis.

1.0.1 The nematic phase (N):

This phase has a high degree of long range orientational order of the molecules, but lacks positional order. Thus, this fluid phase differs from the isotropic liquid in that the molecules are spontaneously oriented with their long axes approximately parallel. The average orientation or preferred direction of the molecules is represented by an apolar unit vector called the director (n). Even though the preferred direction of the molecules varies from point to point in the medium, a uniformly aligned sample is optically uniaxial with the optic axis along n, positive and strongly birefringent. Owing to its fluidity, the molecules can easily slide past one another while still retaining parallelism. **A** schematic diagram of the structure of this phase is shown in figure 1.1.

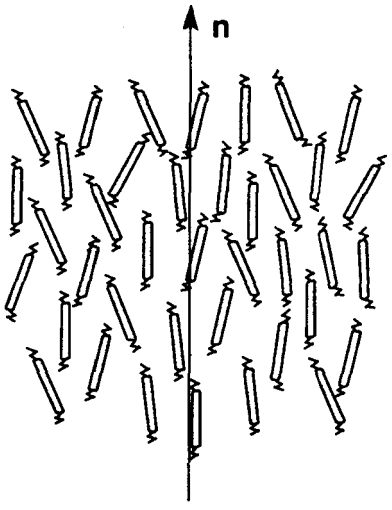


Fig 1.1 : A schematic representation of the structure of nematic phase.

1.0.2 The cholesteric phase (N^*):

If a compound composed of optically active molecules forms a nematic phase or if a nematic phase is doped with a chiral compound, then the structure as a whole becomes chiral and forms a helical twist [2]. The phase can be described as being made up of nematic planes helically piled over one another so that the director is rotating uniformly about the director normal. This helical nematic structure is called a cholesteric phase. Figure 1.2 shows the molecular arrangement in the cholesteric phase.

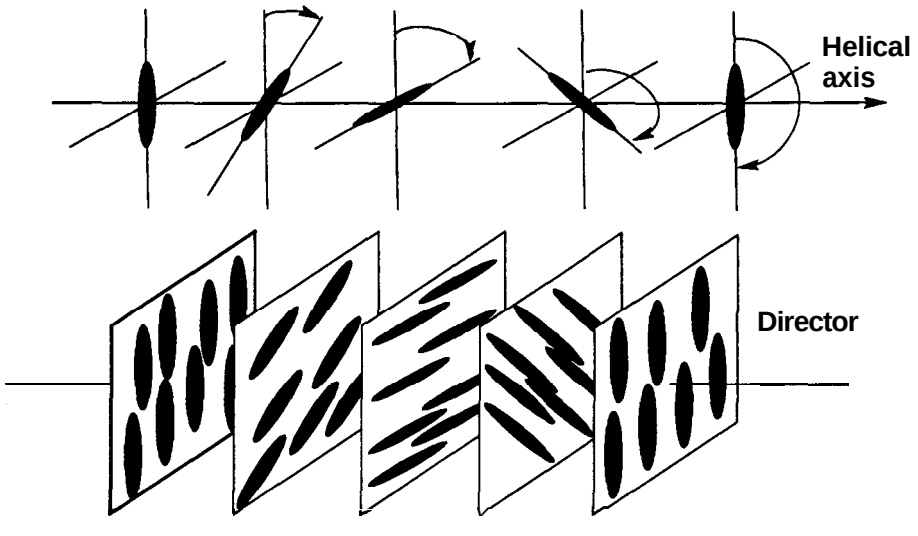


Fig 1.2 : A schematic representation of arrangement of molecules in the cholesteric phase.

The helical twist may be right-handed or left-handed depending on the molecular conformation of the constituent molecules. The pitch of the helix is often of the order of wavelength of visible light and hence is responsible for the medium to exhibit unique optical properties, viz., selective reflection of circularly polarized light. The rotatory power of the N* phase is about a thousand times greater than that of an ordinary optically active substance. The cholesteric phase is optically uniaxial and negative with the optic axis along the helical axis.

1.0.3 The blue phases (BP):

These phases often appear over a narrow range of temperature (< 1°C) between cholesteric and isotropic liquid for N* phase of relatively short pitch (< 5000 Å). The first observation of the blue phase has been attributed to Reinitzer [3]. These are thermodynamically stable phases. Three distinct blue phases have been identified: BP I, BP II and BP III, which occur in the same order with increasing temperature. Optical bragg reflection studies show that BP I has a body-centered cubic lattice, BP II has a simple cubic lattice and BP III is probably amorphous.

1.0.4 The smectic phases (Sm):

Smectic liquid crystals are characterized by their stratified structures with a well-defined interlayer spacing, which can be measured by x-ray diffraction studies [4]. The first x-ray evidence for the layered structure was obtained by Friedel [4]. Thus, smectic liquid crystals are more ordered than nematic liquid crystals and they occur at temperatures below the latter. A variety of molecular arrangements are possible within the stratification leading to different types of smectic liquid crystalline modifications.

1.0.4.1 The smectic A phase (Sm A):

This phase has a layered arrangement with the molecular long axes being perpendicular to the planes of the layers. As a consequence, the layer spacing in this phase is very close to the full length of the constituent molecules, which is confirmed by x-ray diffraction studies [5]. Within each layer, the centers of gravity show a

short-range order and the molecules are able to rotate freely about their long axes. Hence this phase can be looked upon as a two-dimensional liquid. This phase is optically uniaxial with the optic axis normal to the plane of the layers and has a D_∞ symmetry. This smectic modification possesses the least order, though it is very much more viscous than the nematic phase. The fluid property of this phase has been attributed to the weak interlayer attractions as compared to the lateral forces between the molecules. In any phase sequence which includes Sm A, this phase precedes all other smectic phases upon either cooling the isotropic liquid or the nematic phase. **A** schematic diagram representing the molecular arrangement in this phase is shown in figure 1.3.

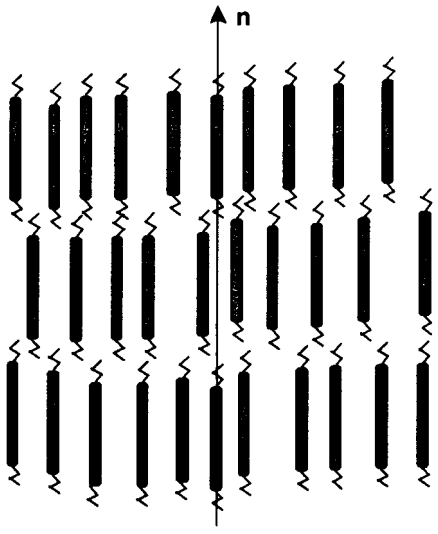


Fig 1.3 : A schematic representation of the structure of Sm A phase.

1.0.4.2 The smectic C phase (Sm C):

This phase is a tilted analogue of the Sm A phase, ie., the long axes of the molecules are tilted with respect to the layer normal. Each layer in this phase is again a two-dimensional liquid with the molecules being arranged randomly within the layers. There is no long-range correlation, except for the tilt direction, between the layers. This phase is optically biaxial with the optic axis being tilted with respect to the layer normal. The tilt angle in this phase has been shown to vary with temperature and it often increases with decreasing temperature in a uniform way. From x-ray studies [6-8] it is evident that the layer thickness in this phase is considerably less

than the molecular length. The symmetry elements of this phase correspond to point group C_{2h}. Figure 1.4 shows schematically the arrangement of molecules in this phase.

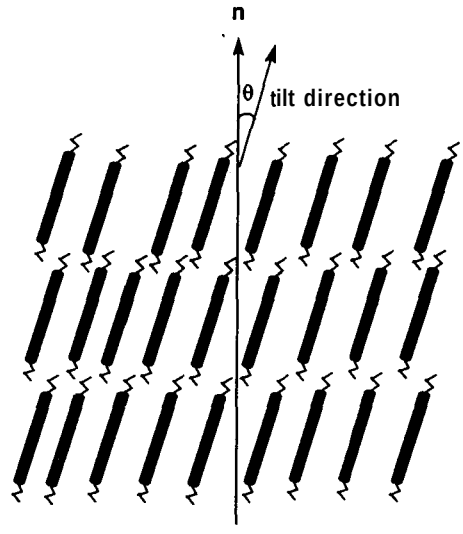


Fig 1.4 : A Schematic diagram showing the structure of Sm C phase.

1.0.4.3 The chiral smectic C phase (Sm C^*) and ferroelectricity:

This phase is an interesting modification of the Sm C phase, with a twist axis normal to the layers. The possibility of formation of such a structure by the addition of optically active molecules to the ordinary Sm C phase was envisaged by Saupe [9]. However, the first recorded observation of this chiral phase in pure chiral compounds has been attributed to Helfrich and Oh [10]. Figure 1.5a represents the structure of Sm C* phase. Some of the optical properties like the propagation of light along the twist axis ***etc.,*** are identical to those of a cholesteric phase. In the year 1975 Meyer ***et*** al. [11] based on symmetry arguments predicted that the Sm C* phase ought to be ferroelectric and indeed showed that 4-n-decyloxybenzylidene-4'-amino-2-methylbutylcinnamate had ferroelectric properties. A brief summary of their arguments is given below.

For a Sm C phase composed of non-chiral molecules the space symmetry elements are:

a. **A** mirror plane
b. **A** two-fold axis of rotation
c. A center of symmetry.

Thus the symmetry is classed as C_{2h}. In the Sm C^* phase on the other hand, the molecules are tilted, and their rotation about their long axes is biased. Since the molecules are chiral the mirror plane of the ordinary Sm C structure is absent. The only symmetry element that remains is a two-fold axis parallel to the layers and normal to the long molecular axis. This low local symmetry forces the transverse dipole moments of the molecules to align along the C_2 axis perpendicular to the tilting plane, leading to a macroscopic polarization within the smectic layer ie., in Sm C* phase each layer is spontaneously polarized. The presence of a spontaneous polarization in smectics is assumed to be due to a time-dependent coupling of the lateral components of the dipoles of the individual molecules with the chiral environment. Since the structure has a twist about the layer normal, the tilt and hence the polarization direction rotate from one layer to the next (fig 1.5a).

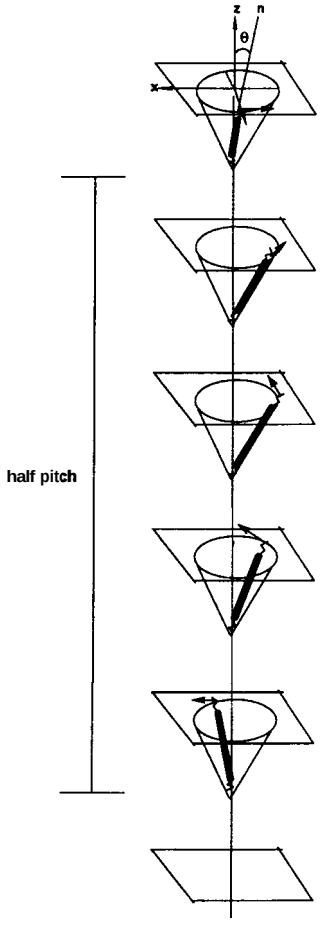


Fig 1.5a : A schematic diagram of the helicoidal ferroelectric phase (after Fukuda *et al.* [13]).

As a consequence, the net polarization averages to zero. However, when an electric field E is applied normal to the helical axis, the helix gets distorted and above a

critical field, the helix is completely unwound resulting in a net spontaneous polarization. Under such conditions the molecules are aligned in a plane perpendicular to E with a tilt θ with respect to the layer normal (fig 1.5b).

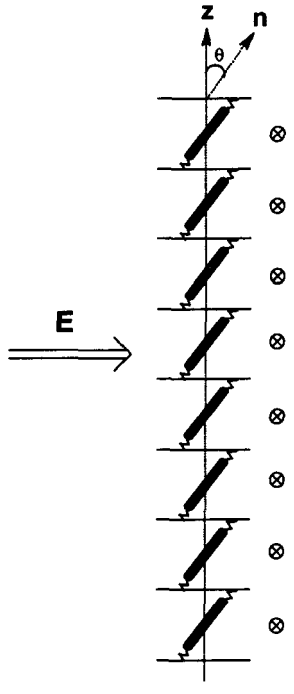


Fig 1.5b : A diagrammatic representation of the unwound ferroelectric phase on application of an electric field E normal to the helical axis.

When the field is reversed, the direction of polarization reverses and due to the coupling of polarization and tilt, the orientation of the molecule switches from +θ to -θ, thus leading to ferroelectricity of the medium. It is important to note that in sufficiently thin cells, the helix can also be unwound by the surface effects, when the axis is parallel to the substrate plates[12]. These surface stabilized ferroelectric liquid crystal (SSFLC) cells inturn exhibit bistable switching on reversing the sign of an applied electric field as shown in figure 1.5c.

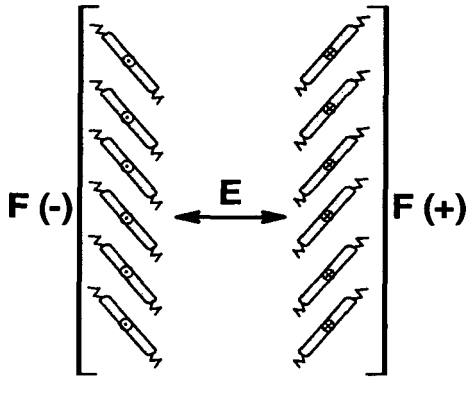


Fig 1.5c : Diagram showing the bistable switching in the ferroelectric phase.

The macroscopic polarization within the smectic layer can be represented by the equation:

$$P = P_0 \frac{z x n}{|z \times n|}$$

Where z is a unit vector parallel to the layer normal and n is the director; z coincides with n when the tilt angle θ becomes zero. The reversal of the tilting sense results in a reversal of the polarization sense.

1.0.4.4 The antiferroelectricsmectic C phase (Sm C^*_A):

This phase was discovered by Chandani *et* ***al.*** [13] in 4-(1-methylheptyloxycarbonyl)phenyl-4'-n-octyloxybiphenyl-4-carboxylate (MHPOBC) in the year 1989. This phase also exhibits a helicoidal macrostructure similar to that of a ferroelectric phase except that the molecules tilt in almost the same direction but in opposite sense on moving from one layer to the other.

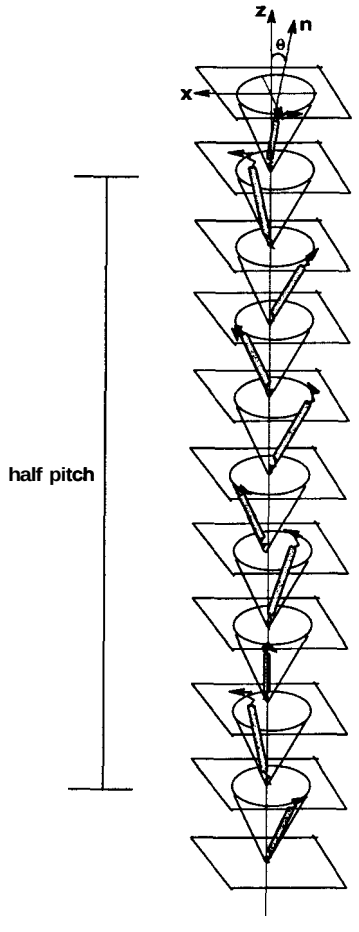


Fig 1.6a : Schematic representation of the helicoidal antiferroelectric phase (after Fukuda *et al.* [13]).

As a result of this the spontaneous polarization in the neighbouring layers also point in opposite direction thereby cancelling each other. The proposed helical structure of this phase is shown in figure 1.6a. Under the influence of low electric fields, the helix unwinds and unlike in ferroelectrics, the net polarization still remains zero due to the molecular arrangement. Hence no switching is seen (fig 1.6b).

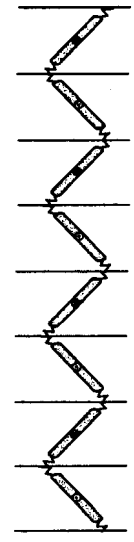


Fig 1.6b : Schematic depiction of the unwound antiferroelectric phase under low electric field (after Fukuda *et al.* [13]).

However, at higher fields (greater than the threshold field), transitions between antiferro- and ferroelectric phases are induced leading to tristable switching [14-17]. Figure 1.6c shows the tristable states of the antiferroelectric phase.

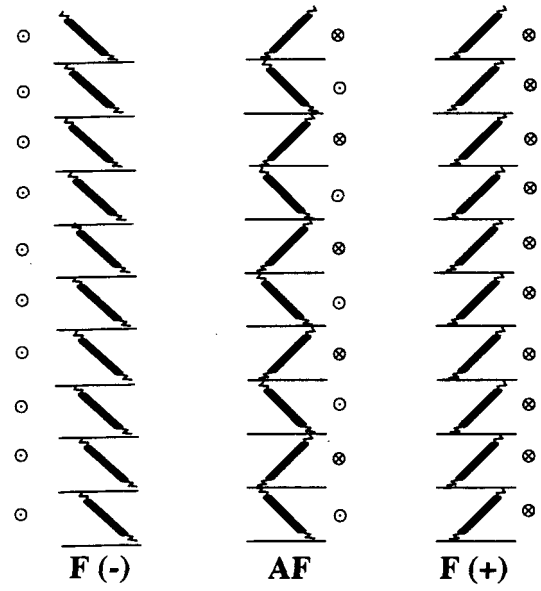


Fig 1.6c : Schematic diagram of tristable switching in the antiferroelectric phase; F (-)↔AF↔F (+); F and AF refer to ferro- and antiferroelectric states, respectively (after Fukuda ***et al.*** [13]).

1.0.4.5 The ferrielectric phase (Sm C^*_γ):

This phase exists between Sm C* and Sm C^*_A phases, hence it possesses an intermediate structure. On the basis of x-ray, conoscopy, rotatory power, dielectric and electrooptic measurements [18] it was shown that this phase has an intermediate spontaneous polarization and tilt angle compared with those of the Sm C* and Sm C^*_A phases and hence is a helical ferrielectric phase. Upto now three ferrielectric phases have been found experimentally with different intermediate structures. Several model structures were proposed for this phase [18]. The model proposed by Roy and Madhusudana [19] which is called the clock-model or the xy-model explained all the experimental observations obtained from conoscopy, dielectric and electrooptic measurements. From the conoscopic observations it was uniequivocally established that this phase has a helicoidal structure and this disproves the assumption of the Ising character of the orientational order parameter that was previously proposed for this phase by Fukuda et al. [18]. Both dielectric and electrooptic measurements detect modes with the relaxation frequencies typical of the Goldstone mode [20] which again indicates an xy-type behaviour of the orientational order parameter in this phase. Most importantly, the resonant x-ray scattering studies [21] have clearly shown that only the discrete xy-model is realistic and describes the structure of the ferrielectric phase, thus providing conclusive experimental evidence in favour of the xy-model.

1.0.4.6 The chiral smectic C alpha phase (Sm C^*_α):

This phase has a very complex structure. Several structural models have been proposed and numerous experimental results are reported for this phase in the literature, but its exact structure has not yet been determined. Recently, it was concluded that the model proposed by Žekš and Čepič [22,23] was in good agreement with the experimental results [24,25]. According to their model, this phase has a helical structure, with a short pitch and a phase difference α between the two nearest layers. The azimuthal angle α is sensitive to temperature ie., it is weak at low temperatures (ferroelectric-like phase), increases beyond $\pi/2$, and finally reaches values close to π (antiferroelectric-like phase) at high temperatures. This kind of structural fragility was very clearly observed in the experimental studies. X-ray

studies showed that the molecules are tilted and the tilt angle is constant through all the layers. Figure 1.7 shows a schematic representation of the structure of the Sm C^*_α phase.

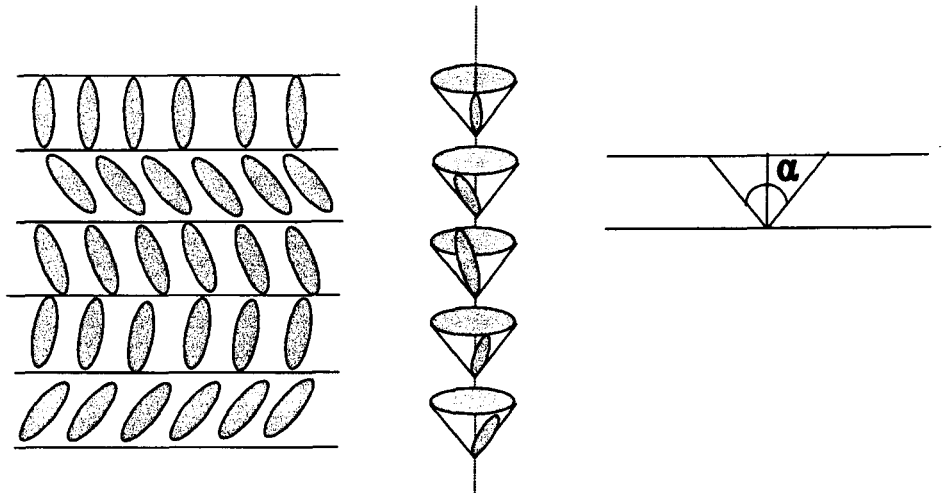


Fig 1.7 : Schematic representation of the structure of Sm C^*_α phase [after Žekš and Čepič [22]).

1.0.5 The twist grain boundary (TGB) phases:

These phases were found to mediate the $N^*\leftrightarrow$Sm A, isotropic$\leftrightarrow$Sm A and $N^*\leftrightarrow$Sm C* transitions, resulting in the occurrence of TGB_A and TGB_{C^*} phases. Based on the predictions made by de Gennes [26], Renn and Lubensky [27] worked out a theoretical model for these phases. However, the credit for the discovery of the existence of TGB_A phase in some propiolate derivatives has been attributed to Goodby *et al.* [28,29].

1.0.5.1 The twist grain boundary smectic A phase (TGB_A):

At a normal transition from N* to a Sm A phase, the helical ordering of the N* phase collapses to give the layered structure of the Sm A phase. However, for a transition mediated by a TGB phase, the molecules compete between the formation of a helical structure due to their chiral packing requirements and the lamellar or layered structure. As a consequence, the molecules relieve this frustration by forming a

helical structure, in which the axis of the helix is perpendicular to the long axis of the molecules, along with a layered structure. Since the two structures are incompatible, their coexistence is made possible by the formation of an array of screw dislocations, which subsequently forms grain boundaries in the phase. Hence in a TGB_A phase, the Sm A blocks rotate with respect to one another by the screw dislocations, forming a helical structure. Figure 1.8 depicts the structure of the TGB_A phase.

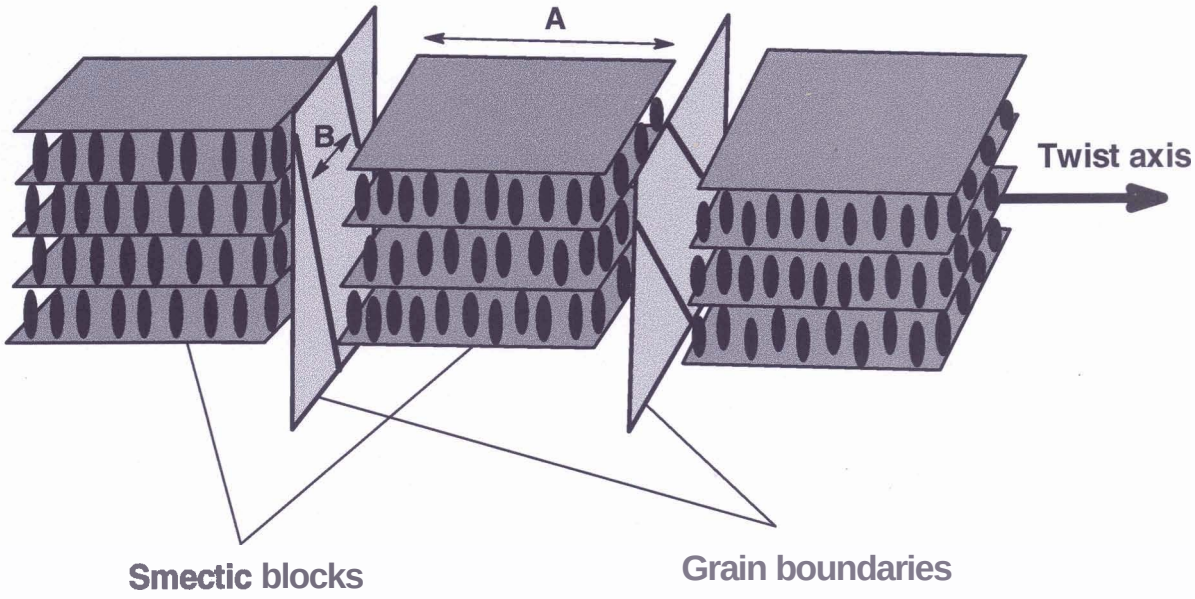


Fig 1.8 : A schematic representation of the structure of TGB_A phase; A is the block size; B is the spacing between screw dislocations within the grain boundary (after Goodby *et al.*[28]).

The pitch of the helix falls within the order of wavelength of visible light. Hence analogous to the cholesteric phase, this phase also exhibits properties like the selective reflection of light.

The TGB phase can exhibit different modifications like TGB_C, TGB_{C*} phases etc., depending on the structure within the smectic blocks. The structure of the TGB_C phase is similar to that of a TGB_A phase except that the molecules within the smectic blocks are now tilted with respect to the layer normal. Experimentally it was observed that the smectic layers are tilted with respect to the grain boundary by an

angle, which is approximately equal to the Sm C tilt angle [30,31]. Figure 1.9 shows the structure of this phase.

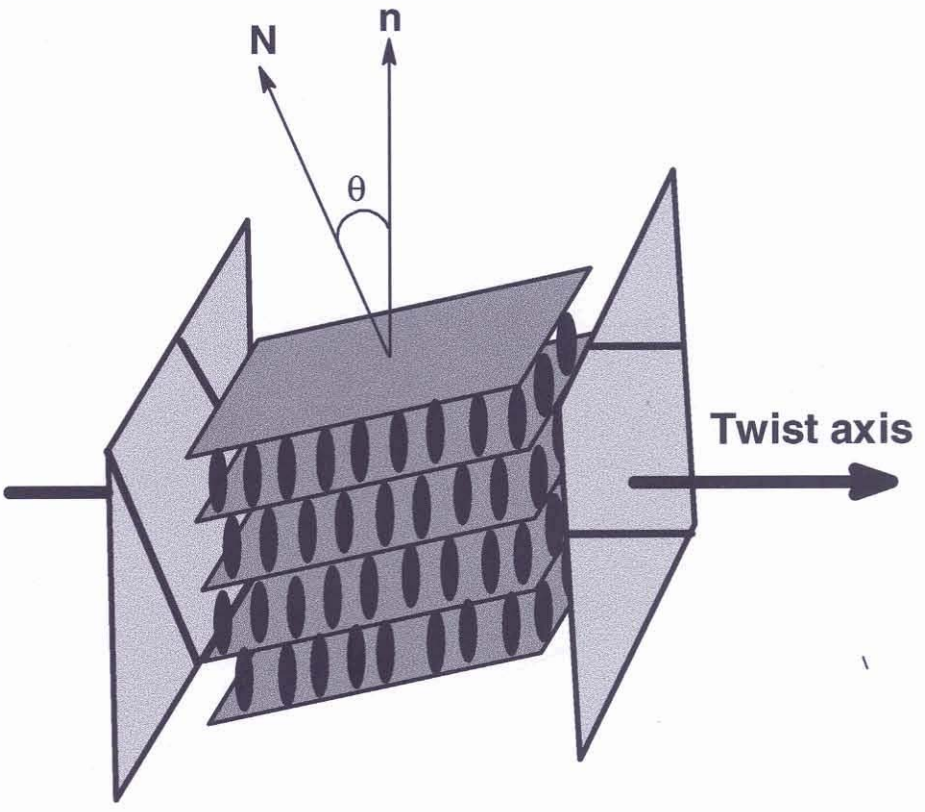


Fig 1.9 : Schematic diagram of the structure of TGB_C phase; N is the layer normal and θ is the angle by which the smectic layers are tilted with respect to the grain boundary (after Nguyen *et al.* [31]).

The TGB_{C^*} phase has a Sm C^*-like blocks in which the tilt direction has a helical arrangement about the layer normal [32].

1.0.5.2 The undulated twist grain boundary smectic C* phase ($UTGB_{C^*}$):

This new chiral helical phase was discovered by Pramod et *al.* [33] in the year 1997 in a binary mixture of the chiral compound 4-(2'-methylbutyl)phenyl-4'-n-octylbiphenyl-4-carboxylate and 2-cyano-4-n-heptylphenyl-4'-n-pentylbiphenyl-4-carboxylate which have very similar lengths and molecular structures. The structure of this phase is far more complicated than the TGB_A and TGB_C phases. In this phase

the smectic blocks rotate about each other forming a helical structure. Within each smectic block, the tilt direction of the molecules precesses about the layer normal to form a smectic C^*-like arrangement resulting in a TGB_{C^*}-like structure. In addition to this, the grain boundaries have two-dimensional undulations along two mutually orthogonal directions in view of the uniaxial symmetry of the TGB structure, thus forming a square grid. A schematic diagram of the proposed structure for this new phase is shown in figure 1.10. All the grain boundaries undulate along the same two directions in order to maintain uniformity of the block thickness. This proposed structure is rather non-uniform and is reminiscent of the blue phases exhibited by short-pitched cholesterics. However unlike them this is anisotropic and does not have a cubic symmetry.

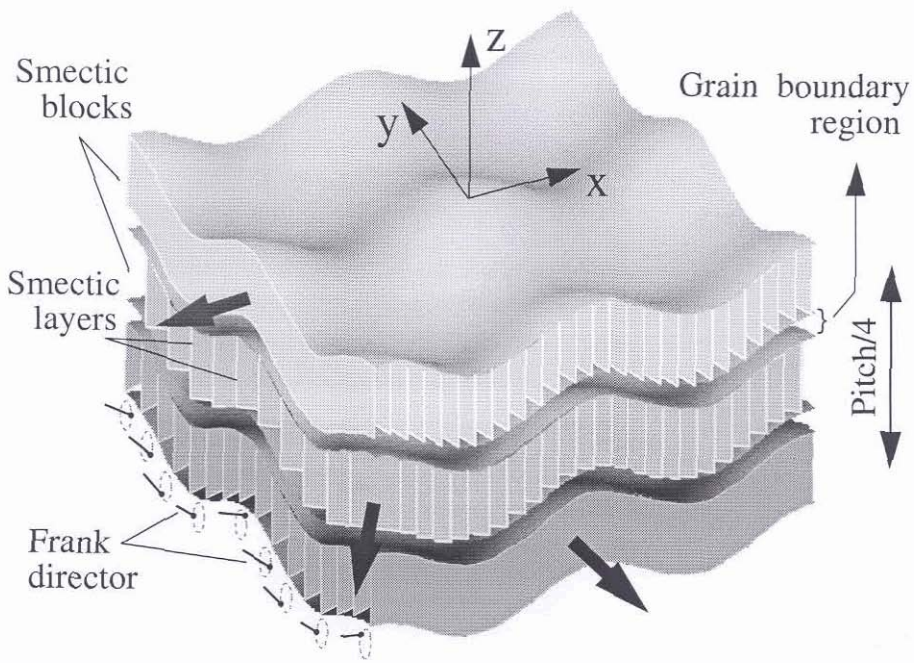


Fig 1.10 : A schematic representation of the proposed structure for the $UTGB_{C^*}$ phase. The shaded area represents the two-dimensionally undulated grain boundary region. The smectic layer normals (large arrows) rotate from block to block. Within each block the Frank director precesses along the layer normal direction as represented by the nails. (after Pramod et *al.* [33]).

1.1 Mesophases of compounds composed of banana-shaped or bent-core molecules:

Until recently it was believed that for a compound to exhibit ferroelectricity and antiferroelectricity, tilted association of the chiral molecules into a smectic layer reducing the overall symmetry of the liquid crystal was an essential requirement. However, in the year 1996 Niori et *al.* [34] disproved this myth by reporting a distinct ferroelectric smectic liquid crystal formed from a compound composed of achiral banana-shaped or bent-core molecules. The origin of chirality in such systems has been ascribed to the spontaneous symmetry breaking of achiral symmetry in bulk liquid crystal, which arises from the sterically induced packing of these achiral molecules. According to them [34] the packing is such that the molecules are arranged in layers and are all aligned in the direction of bending. As a consequence of this, spontaneous polarization appears parallel to the layer and switches on reversal of an applied electric field thus giving rise to ferroelectricity. This is the first obvious example of ferroelectricity exhibited by an achiral smectic phase and has been attributed to the C_{2v} symmetry of the packing of the banana-shaped molecules into a layer. Prior to the discovery of ferroelectricity in such systems by Niori et *al.* [34], Matsunaga et *al.* [35,36] had synthesized a few compounds with achiral bent-core molecules, which they found were forming smectic layers. However, they did not pursue this further in analyzing their structure and properties. Weissflog et *al.* [37] and Heppke et *al.* [38] discovered antiferroelectric switching behaviour in one of the compounds synthesized by Matsunaga et *al.* Link et *al.* [39] confirmed this by electrooptical investigations on freestanding films and on sandwich preparations.

As a consequence of special packing of these bent-core molecules, there is a possibility of occurrence of various smectic modifications with C_{2v}, C_2, C_{1h} and C_1 symmetry [40] giving rise to ferro-, fem- or antiferroelectric properties, which may find useful applications in the field of display technology.

Miscibility studies conducted on the smectic mesophases exhibited by these compounds with those exhibited by the calamitic liquid crystals showed that the two were not miscible with each other. Therefore these mesophases were described using a different nomenclature consisting of the code letter B as B_1, B_2, B_3 *etc.*, which was suggested at the workshop on banana–shaped liquid crystals held in Berlin in the year

1997, where the letter B refers to the bent- or bow- or banana shape of the molecules. A general molecular space-filling model of a compound composed of banana-shaped molecule is shown in figure 1.11.

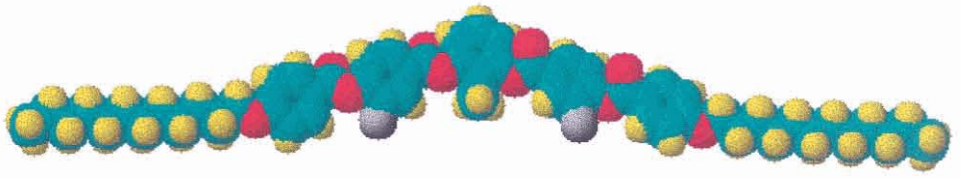
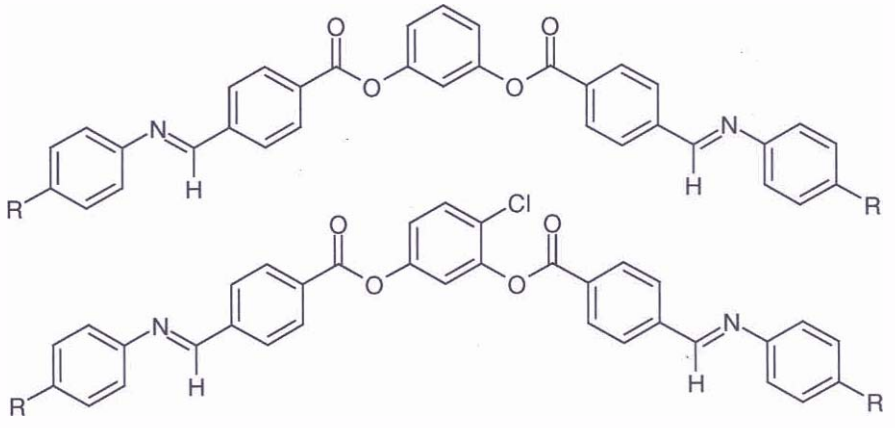


Fig 1.11 : A molecular s p a c e - f i i model of a compound composed of banana-shaped molecule.

As of now, seven different mesophases have been experimentally reported (B_1, B_2…..B_7), out of which the structural details of only five mesophases have been understood to some extent. However, except for the B_2 phase the structures of all the other mesophases are still not clear. In the following section, a brief description of the structures of the mesophases exhibited by the compounds composed of banana-shaped molecules is presented.

1.1.1 The B_1 phase:

This phase also designated as SmA^1_b [41,42] or X_{B1} [38] was first observed in the lower homologues of the compounds having the general molecular structure:



A detailed x-ray analysis was performed in order to understand the molecular arrangement in this phase. The x-ray pattern of an oriented sample showed four sharp inner reflections and a broad outer reflection. Analysis of the diffraction profile

obtained for this phase indicated that they were similar to those observed for the frustrated smectic phase of a polymer [43,44]. This suggested that B_1 phase was a frustrated smectic phase. The spacing of the inner reflections and their diffraction geometry could be well explained by considering a two-dimensional rectangular lattice with well defined parameters a and c. The c-axis represents layer thickness whose length corresponds to the molecular length and the a-axis along which the frustration viz. unusual density modulation took place corresponds to the bent-direction of the molecules. A schematic diagram of the frustrated structure of this phase is illustrated in figure 1.12.

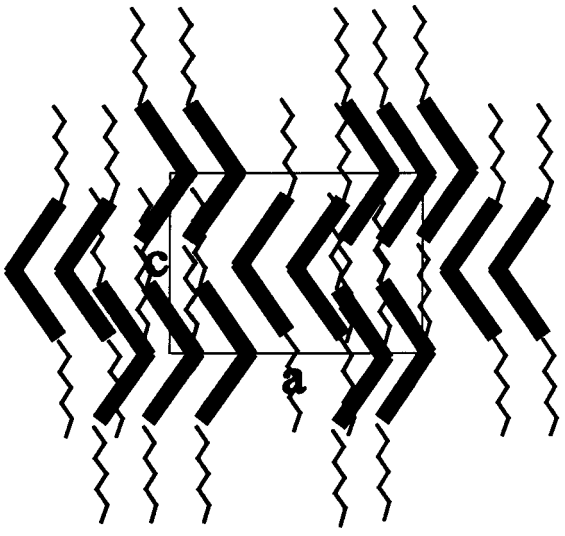


Fig 1.12 : A schematic representation of the proposed structure for the B_1 phase (after Watanabe et al. [42]).

The length of the a-axis indicated that each unit is composed of about 8-10 molecules on an average, which implies the presence of 4 or 5 molecules in each frustrated domain. The above proposed model is fully based on only the x-ray diffraction pattern. However, further experiments have to be carried out in order to fully understand the structure of this phase.

1.1.2 The B_2 phase:

Among all the seven identified phases, the structure of this phase has been understood in greater detail. This phase has also been designated as S_{X1} [45], SmX_1 [46], M_1 [47], X_{B2} [38] or $SmCP_A$ [39] in the literature. One of the interesting aspects of this phase is its ability to exhibit ferroelectric switching, which was discovered by

Niori et *al.* [34] in the year 1996. It was this special feature of the B_2 phase, which motivated the scientists to explore its structure in greater detail. Later, in the year 1997 Weissflog et *al.* [37] and Heppke et *al.* [38], conducted electrooptic studies on the compounds synthesized by Matsunaga et *al.* [35,36,48] and found that they exhibited two current peaks during a half period of a triangular voltage, which clearly indicated antiferroelectric switching behaviour. It was Link et *al.* [39] who demonstrated beautifully that this phase is antiferroelectric by conducting similar experiments on freestanding films and on sandwich preparations and proposed a structural model for this phase based on their experimental results. The chirality of this system has been explained using a model as shown in figure 1.13.

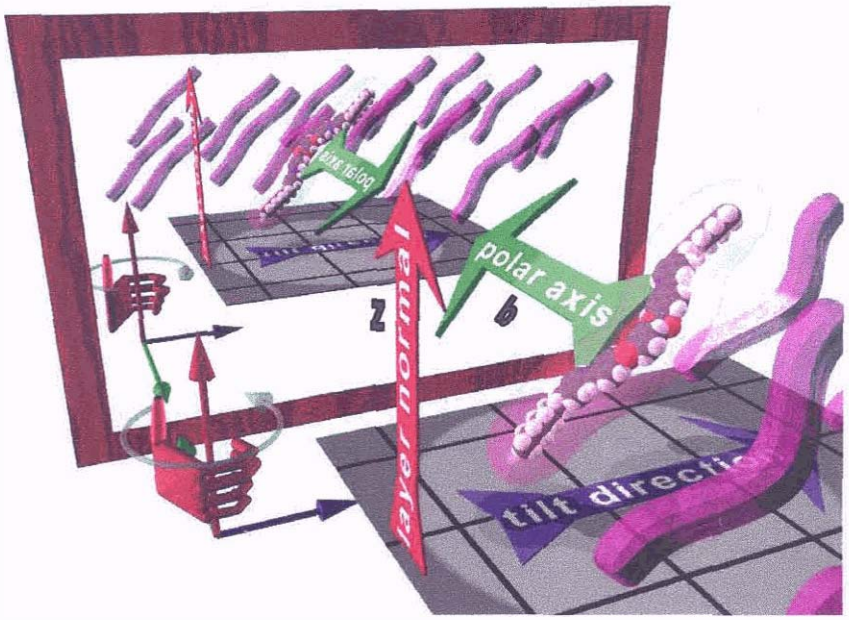


Fig 1.13 : A schematic representation of the proposed structure for the B_2 phase. (after Heppke and Moro [49]).

According to them, due to the bent-shape of the molecules, a special sterically induced packing is favoured in each layer where the molecules are arranged with their molecular axis tilted with respect to the Layer normal z and their ferroelectric polar ordering being oriented in the same direction there by defining a polar axis b. As a result, there exists a net polarization P_b normal to the tilt direction and the layer normal in each layer. This kind of an ordering implies the existence of two equivalent layer structures with antiparallel polar axis, which are non-superimposable mirror images of each other. Therefore despite the fact that the individual molecules are

achiral, the layer as a whole is chiral. On moving from one layer to the other the molecules tilt to different extents there by forming a macroscopic helical structure.

Since the chirality arises from the arrangement of molecules within the layers and not due to the molecular chirality, two types of antiferroelectric equilibrium states are equally probable:

(a) Antiferroelectric-racemic or synclinic antiferroelectric phase, in which the polar direction alternates from layer to layer retaining the tilt sense of the molecules in the same direction.

(b) Antiferroelectric-chiral or anticlinic antiferroelectric phase, in which the tilt direction as well as the polarity alternate from layer to layer.

Under the influence of sufficiently high electric fields, both the antiferroelectric states were found to switch to their corresponding ferroelectric states as shown in figure 1.14

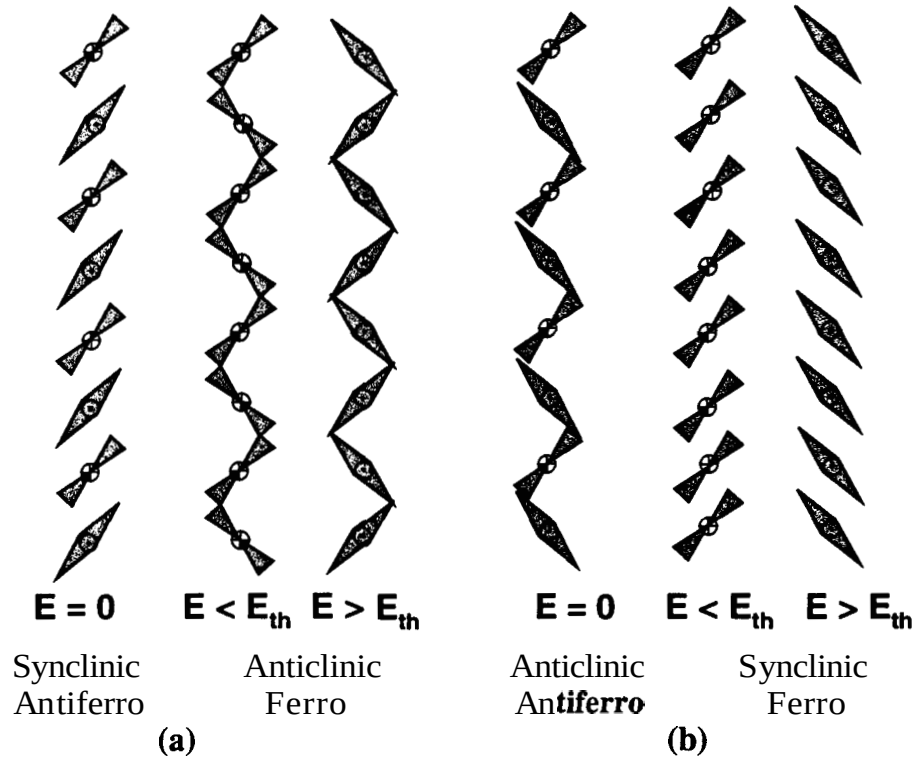


Fig 1.14 : (a) Schematic representation of the arrangement of the molecules in the racemic state at zero applied electric field (E = 0) and in the corresponding ferroelectric states (E_{th} = threshold field). (b) Arrangement of the molecules in the homogeneously chiral state at zero field and in the corresponding ferroelectric states (after Link et al. [39]).

1.1.3 The B_3 phase:

This phase is a higher ordered non-tilted biaxial smectic hexatic B phase [41], which appears at a lower temperature than the B_2 phase. This phase is also designated as SmX_2 [46,50], Hex B_b [41] or XB_3 [38]. The hexatic nature of this phase has not yet been confirmed. X-ray pattern of a non-oriented sample showed a number of strong reflections in the wide angle region, which clearly pointed to the fact that it had a crystalline structure [37]. The electrooptic studies conducted on this phase [50] showed the existence of ferroelectric switching in this phase. Watanabe *et al.* [51] reported a SHG (second harmonic generation) activity in this phase which, however could not be confirmed [52]. The exact structure of this phase is yet to be investigated.

1.1.4 The B_4 phase:

This phase, also designated as SmX_3 [50] or Sm blue [41,38] appears below B_3 phase on cooling. This phase appears more or less like a glassy state with a characteristic blue colour. The origin of this blue colour [45] could be explained by considering a selective Bragg reflection arising from the two domains of the right and left handed helices. Therefore it can be concluded that in a B_4 phase, there is a spontaneous formation of helical domains of both handedness. C^{13} NMR studies clearly indicated a twisted molecular conformation (conformational chirality) in this phase, the stabilization of which could be interpreted as a consequence of the formation of a helical structure. X-ray diffraction pattern indicated a two-dimensionally ordered packing of molecules in this phase, with a decrease in the long-range order as compared to that of the B_3 phase. Similar studies on homeotropically aligned sample confirmed the parallel orientation of the helical axis with respect to the smectic layers. Based on the above experimental results Sekine *et al.* [28,53,54] proposed a TGB-like twisted structure for this phase as shown in figure 1.15.

This phase was found to be SHG-active even in the absence of an external electric field, which indicated the spontaneous non-centrosymmetric ordering of the molecules [51,52].

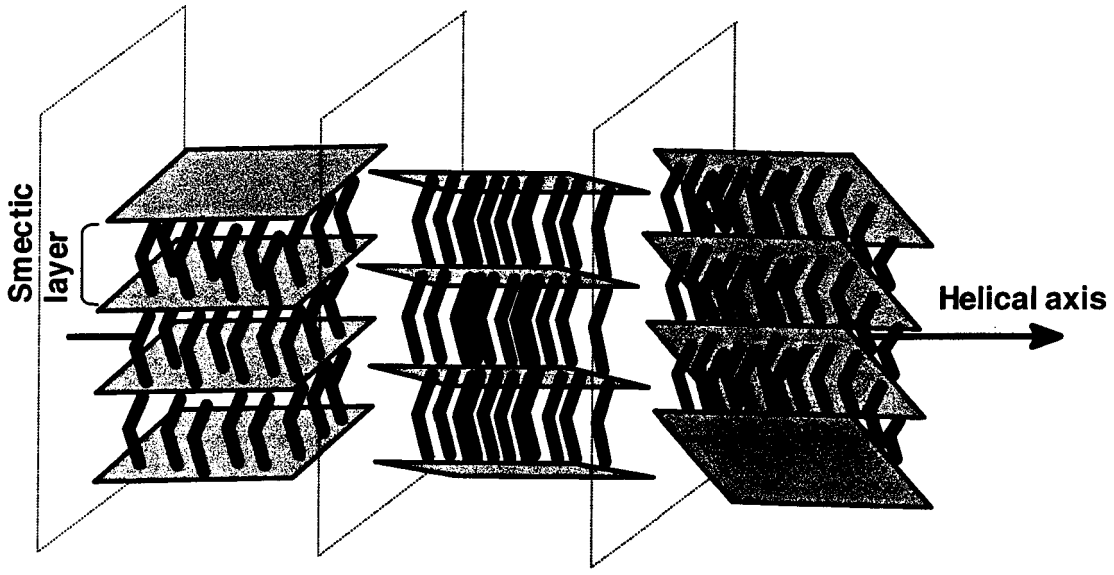


Fig 1.15 : A schematic representation of the proposed structure for the B_4 phase (after Sekine *et* al. [41]).

1.1.5 The B_5 phase:

This phase is also designated as the M_2 phase. According to a recent survey, this phase has been found in three 2-methyl resorcinol derivatives [47]. Microscopic textural observations showed a very small difference in the textures between B_5 and the B_2 phase. However, the x-ray patterns of the two were shown to be different. The patterns [47] of the oriented samples in the B_5 phase showed an additional scattering consisting of three maxima on the equator, which indicated density waves perpendicular to the layer normal. The periodicities of these were found to fit well into a two-dimensional rectangular cell, with parameters a and b indicating the existence of a short-range order within the layers. This phase was found to show an optical response comparable with that of the B_2 phase. However, quantitative measurements could not be made because of the relatively high conductivity of the samples.

1.1.6 The B_6 phase:

The structure of this mesophase has been identified by x-ray diffraction studies. The diffraction pattern of an oriented sample [37] indicated that this phase has a tilted smectic structure with tilt angle $\approx 30°$ and without an in-plane order. The layer

spacing was found to be smaller than half-length of the molecules, which indicated an intercalated structure. Diffused lines corresponding to a period ≈ 4.0nm was observed, which is caused by rows of molecules that are non-correlated to each other. **A** schematic diagram of the probable molecular organization in this phase is shown in figure 1.16

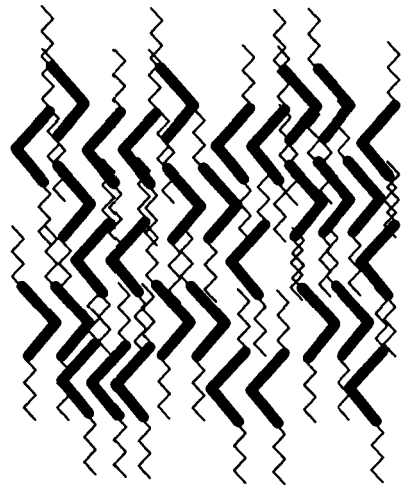


Fig 1.16 : A diagrammatic representation of the probable molecular arrangement in the B_6 phase (after Weissflog *et al*. [37]).

1.1.7 The B_7 phase:

The structure of this phase is still unresolved. This phase has been found in some nitro substituted banana-shaped compounds [37,55]. The x-ray pattern of a non-oriented sample shows several sharp reflections in the small angle region and a diffused reflection in the wide angle region, indicating the absence of an in-plane order. But the position and intensities of the reflections are quite different to those of the B_2 phase. One of the interesting aspects of this phase was the unusual microscopic texture exhibited by it on cooling the isotropic phase. Frequently, spiral and double-spiral germs or circular domains with equidistant stripes were found to be formed from the isotropic liquid. The circular domains which grew like a spiral were analogous to those found in cholesteric or Sm C* phases [56]. On further cooling the one-dimensional periodic patterns were transformed to two-dimensional ones thus giving rise to very complex and beautiful optical textures. These textural observations point to the possibility of a helicoidal structure in this phase. The actual reason behind the origin of the helix in this phase is still not clear. This phase was

found to show electrooptical switching at relatively high voltages. Further detailed investigations have to be carried out in order to deduce the structure of this phase.

1.2 Applications of liquid crystals:

It was not until the mid fifties of the last century that efforts were made to develop applications for these materials. During this period a large number of cholesteric liquid crystals, which find application as temperature sensors were discovered. As a consequence, application of these materials to medical diagnosis, electronic component testing, and aerodynamic structure analysis became feasible. Followed by these discoveries, scientists began to explore the electro- and magnetooptic characteristics of nematic and cholesteric liquid crystals, which resulted in the discovery of dynamic scattering from which the use of liquid crystals in practical electronic displays became evident. Some of the common applications of liquid crystals have been summarized below.

1.2.1 Display applications:

The main application of low molecular mass liquid crystals is in electronic displays. The discovery of dynamic scattering in nematic liquid crystals [57] opened a whole new area of electronic display technology. Today, liquid crystals, which exhibit either this mode of operation or one of the field-effect modes, are used in displays for watches, clocks, calculators, and various digital panel meters. The twisted nematic cells with a twist angle near 90° [58] dominate the commercial production of displays. They are also used as display elements above active matrix backplanes [59] for complex graphics panels. In twisted nematic displays, there exists a possibility for the twist to form either a left- or right-handed helix. However in practice, one sense of twist is selected by adding a small concentration of a chiral additive into the nematic liquid. In order to form a uniformly twisted and tilted structure throughout the cell, the twist direction chosen [60] must be related to the direction of surface tilt at each cell wall.

Ferroelectric liquid crystals have potential applications in complex displays as they show faster switching rates (of the order of microseconds) than the conventional nematic based displays. The device uses a chiral smectic C liquid crystal material in the bookshelf or chevron structure in which the spontaneous polarization vector lies perpendicular to the plane of the cell in either up or down direction and can reorient in response to an applied DC voltage pulse. Both the configurations have the same energy and the switched states can be bistable indefinitely. In contrast to the nematic liquid crystal devices, FLCD suffer from a number of characteristic alignment problems. Damage to the alignment can be induced [61] by mechanical shock or vibration of the cell, or through electrically induced movement of the smectic layers. Following the discovery of antiferroelectric liquid crystals, Nippondenso Co., Ltd. and Showa Shell Sekiyu K.K. demonstrated a prototype antiferroelectric liquid crystal display (AFLCD) at the 1989 SAMPE held at Makuhari messe [62]. The principle used in these devices was the electric field induced transition from the antiferroelectric to ferroelectric phase ie., the tristable switching exhibited by the antiferroelectric liquid crystals. In the multiplexing, hysterisis on the positive and negative sides was used alternatively to avoid the dc component summed in the total applied driving voltages [62,63]. Unlike the FLCD, in AFLCD the spontaneous polarization appears when needed and does not exist permanently; hence the switching in this case may not be hampered by the ghost effect or the unnecessarily strong memory effect, which is difficult to erase [62,63,64]. An ideal viewing angle wider than that in SSFLCD can be obtained by the use of bias voltage in these devices. AFLC cells exhibit remarkable property of self-recovery from alignment damage caused by mechanical and thermal shock during an operation. The quasi-bookshelf smectic layer structure in these devices gives a relatively high contrast ratio of 20-30.

1.2.2 Temperature sensors:

Cholesteric liquid crystals exhibit unique property of selective reflection of light in the visible region. It is this property that has been employed in a number of unique temperature sensing applications. One such application is thermal mapping of electronic components [65], in which the component is coated with the liquid crystal material. This technique was employed to determine heat flow and temperature

distribution patterns in operating devices, which otherwise would be difficult and cumbersome if conventional testing methods were employed because of the microscopic size and high density of integrated and monolithic circuits. Cholesteric liquid crystals also find use as a valuable tool for aerodynamic testing [65]. The use of liquid crystals to observe shear stresses in wind tunnel models was first demonstrated by Klein [66] in 1968. In this technique the neat cholesteric material was applied to the surfaces and the boundaries between laminar and turbulent flow was observed as difference in colour in the aerodynamic models. This technique has also been used to visualize two-dimensional temperature patterns developed during thermal non-destructive tests of other aerospace components and structures.

1.2.3 Medical applications:

Thermochromic liquid crystals have found applications in the field of medicine. Cholesteric liquid crystals find use in making disposable thermometers also known as fever strips. The construction of this is based on an indicator strip printed with several different thermochromic materials, each with a slightly different narrow colour play around normal body temperature. That segment which appears bright green in colour indicates the exact temperature. Sharn Inc. [67] produced a modified device structure in which the indicator strip is coated with a thin film of the liquid crystal and is treated such that the temperature is displayed as a narrow colour band that moves continuously across the device. Cholesteric liquid crystals have also been employed in sensing the temperature changes near the skin surface, which is directly related to certain disorders in the body. It was in the year 1964 [68], when for the first time the use of liquid crystals to indicate skin temperature was discovered and now many patents exist in the area. Other medical applications include the use of liquid crystal extensively in the area of oncology [69-74], in diagnosing acute paraproctitis [75] ***etc.***

1.2.4 Laboratory applications:

The fact that the bulk orientation in liquid crystals can be controlled by different methods along with the special combination of orientational order and mobility have led to numerous applications in which these materials are used as anisotropic liquid

solvents. Nematic liquid crystals, in which the molecules can be homogeneously oriented by a magnetic field such that their optic axis is parallel to the field, are employed as anisotropic solvents in nuclear magnetic resonance spectroscopy. This technique provides information regarding the anisotropy of the chemical shift and molecular geometry. A few general reviews of this technique have appeared in recent years [76,77]. The unique anisotropic properties of liquid crystals have also been employed to control and alter the rates of uni- and bimolecular thermal and photochemical reactions [78,79]. This technique is based on the ability of the liquid crystals to control the orientation of solutes, impart constraints on their mobility and remove the randomness of molecular motions and orientations.

Chromatography is one of the most important analytical tools in modern chemical analysis. A combination of the analytical strengths of gas chromatography and the unique structure and shape selective properties of the liquid crystalline phase has led to widespread use of liquid crystals as stationary phases in gas chromatography. Effective and selective separation of positional and geometric isomers can be brought about by the interaction of the solute with the orientational order provided by the anisotropy of the liquid crystal stationary phase. In the year 1963 Kelker [80] described for the first time the use of liquid crystals in gas chromatography. Later in the year 1964 Dewar and Schroeder [81] carried out notable work in this field.

The recent discovery of ferroelectricity and antiferroelectricity in compounds composed of achiral banana-shaped molecules may extend the application of liquid crystals in the field of display technology. Work is in progress in many laboratories throughout the world in order to understand clearly the structure and properties of these mesophases and to use them advantageously in practical devices.

REFERENCES

[1] F.Reinitzer, Monatsh. Chem., 9,4221 (1888).

[2] P.G.de Gennes, The physics of Liquid Crystals, Oxford University Press (1974).

[3] F.Reinitzer, Monatsh. Chem., 9,421 (1888).

[4] E.Friedel, C.R. Hebd. Seanc. Acad. Sci., Paris, 180,269 (1925).

[5] A.de Vries, Mol. *Cryst.* Liq. *Cryst.*, 20, 119 (1973).

[6] A.de Vries, *Pramana,* Suppl., **1**, 93 (1975).

[7] A.de Vries, *Acta* Crystallogr., A25:S135 (1969).

[8] A.de Vries, J.Phys., Paris, 36, C 1-1 (1975).

[9] A.Saupe, Mol. *Cryst.* Liq. *Cryst.*, **7, 59** (1969).

[10] W.Helfrich and C.S.Oh, Mol. *Cryst.* Liq. *Cryst.*, 14, 289 (1971).

[11] R.B.Meyer, L.Liebert, L.Strzelecki and P.Keller, J. de Physique Letters., 36, L-69 (1975).

[12] R.B.Meyer, Mol. *Cryst.* Liq. *Cryst.*, 40, 33 (1977).

[13] A.D.L.Chandani, E.Gorecka, Y.Ouchi, H.Takezoe and A.Fukuda, Jpn. J. Appl. Phys., 28, L1265, (1989).

[14] A.D.L.Chandani, T.Hagiwara, Y.Suzuki, Y.Ouchi, H.Takezoe and A.Fukuda, Jpn. J. Appl. Phys., 27, L729, (1988).

[15] H.Takezoe, J.Lee, A.D.L.Chandani, E.Gorecka, Y.Ouchi, A.Fukuda, K.Terashima and K.Furukawa, Ferroelectrics, 114, 187 (1991).

[16] H.Takezoe, A.D.L.Chandani, J.Lee, E.Gorecka, Y.Ouchi, A.Fukuda, K.Terashima, K.Furukawa and A.Kishi, Abs. 2^{nd} Znt. Symp. on *FLCs.*, Goteborg, P. 026 (1989).

[17] H.Takezoe, A.D.L.Chandani, E.Gorecka, Y.Ouchi and A.Fukuda, Abs. 2^{nd} Znt. Symp. on *FLCs.*, Goteborg, p. P108 (1989).

[18] H.Takezoe, J.Lee, Y.Ouchi and A.Fukuda, Mol. *Cryst.* Liq. *Cryst.*, 202, 85 (1991).

[19] A.Roy and N.V.Madhusudana, Eur. Phys. J. E., 1 , 319 (2000).

[20] P.Mach, R.Pindak, A.M.Levelut, P.Barois, H.T.Nguyen, C.C.Huang and L.Furenlid, Phys. Rev. Lett., 81, 1015 (1998).

[21] S.Sarala, A.Roy, N.V.Madhusudana, H.T.Nguyen, C.Destrade and P.Cluzeau, Mol. *Cryst.* Liq. *Cryst.*, 261, 1 (1995).

[22] B.Žekš and M.Čepič, Liq. *Cryst.*, 14,445 (1993).

[23] M.Čepič and B.Žekš, Mol. *Cryst.* Liq. *Cryst.*, **263**, 61 (1995).

[24] V.Laux, N.Isaert and G.Joly, Liq. *Cryst.*, 26, 361 (1999).

[25] V.Laux, N.Isaert, V.Faye and H.T.Nguyen, Liq. *Cryst.*, 27, 81 (2000).

[26] P.G.de Gennes, Solid State Commun., 10,753 (1972).

[27] S.R.Renn and T.C.Lubensky, Phys. Rev. A., 38,2132 (1988).

[28] J.W.Goodby, M.A.Waugh, S.M.Stein, E.Chin, R.Pindak and J.S. Patel, Nature, London, 337,449 (1989).

[29] J.W.Goodby, M.A.Waugh, S.M.Stein, E.Chin, R.Pindak and J.S. Patel, J. Am. Chem. *Soc.*, 111,8119 (1989).

[30] L.Navailles, R.Pindak, P.Barois and H.T.Nguyen, Phys. Rev. Lett., 74, 5224 (1995).

[31] M.Petit, P.Barois and H.T.Nyugen, *Euro.* Phys. Lett., 36 185(1996).

[32] S.R.Renn, Phys. Rev. A., 45,953 (1992).

[33] P.A.Pramod, R.Pratibha and N.V.Madhusudana, *Curr.* Sci., **73**, 761 (1997).

[34] T.Niori, T.Sekine, J.Watanabe, T.Furukawa and H.Takezoe, J. Mater. Chem., 6, 1231 (1996).

[35] Y.Matsunaga and S.Miyamoto, Mol. *Cryst.* Liq. *Cryst.*, **237**, 311 (1993).

[36] T.Akutagawa, Y.Matsunaga and K.Yashubara, Liq. *Cryst.*, 17,659 (1994).

[37] W.Weissflog, C.Lischka, I.Benne, T.Scharf, G.Pelzl, S.Diele and H.Kruth, Proc. SPIE: Int. *Soc.* Opt. Eng., 3319, 14 (1998).

[38] G.Heppke, D.Krüerke, C.Löhning, D.Lötzsch, S.Rauch and N.K.Sharma, Freiburger Arbeitstagung *Flüssige Kristalle*, Freiburg, Poster P70 (1997).

[39] D.R.Link, G.Natale, R.Shao, J.E.Maclennan, N.A.Clark, E.Körblova and D.M. Walba, Science, 278, 1924 (1997).

[40] H.R.Brand, P.E.Cladis and H.Pleiner, Eur. J. Phys. (B)., 6 , 347 (1998).

[41] T.Sekine, T.Niori, M.Sone, J.Watanabe, S.W.Choi, Y.Takanishi and H.Takezoe, Jpn. J. Appl. Phys., 36,6455 (1997).

[42] J.Watanabe, T.Niori, T.Sekine and H.Takezoe, Jpn. J. Appl. Phys., 37, L139 (1998).

[43] J.Watanabe, Y.Nakata and K.Simizu, J. Phys. *II* (France)., 4,581 (1994).

[44] J.Watanabe and Y.Nakata, Polym. J., 29, 193 (1997).

[45] T.Sekine, T.Niori, J.Watanabe, T.Furukawa, S.W.Choi and H.Takezoe, J. *Mater.* Chem., 7,1307 (1997).

[46] T.Niori, T.Sekine, J.Watanabe, T.Furukawa and H.Takezoe, Mol. *Cryst.* Liq. *Cryst.*, 301, 337 (1997).

[47] S.Diele, S.Grande, H.Kruth, C.Lischka, G.Pelzl, W.Weissflog and I.Wirth, Ferroelectrics, 212, 169 (1998).

[48] H.Matsuzaki and Y.Matsunaga, Liq. *Cryst.*, 14, 105 (1993).

[49] G.Heppke and D.Moro, Science, 279, 1872 (1998).

[50] T.Sekine, Y.Takanishi, T.Niori, J.Watanabe and H.Takezoe, Jpn. J. Appl. Phys., 36, L1201 (1997).

[51] S.W.Choi, Y.Kinoshita, B.Park, H.Takezoe, I.Niori and J.Watanabe, Jpn. J. Appl. Phys., 37,3408 (1998).

[52] F.Kentischer, R.Macdonald, P.Warnick and G.Heppke, Proc. SPIE., 3142, 128 (1997); Liq. *Cryst.*, 25, 341 (1998).

[53] J.W.Goodby, J. *Mater.* Chem., 1, 307 (1991).

[54] H.T.Nguyen, R.J.Twieg, M.F.Nabor, N.Isaert and C.Destrade, Ferroelectrics, 121, 187 (1991).

[55] G.Pelzl, S.Diele, A.Jákli, C.Lischka, I.Wirth and W.Weissflog, Liq. *Cryst.*, 26, 135 (1999).

[56] L.Bourdon, I.Sommeria and M.Kleman, J. Phys. Fr., **43**, 77 (1982).

[57] G.H.Heilmeier, L.A.Barton and L.A.Zanoni, Proc. IEEE., 56, 1162 (1968).

[58] M.Schadt and W.Helfrich, Appl. Phys. Lett., 18, 127 (1971).

[59] F.C.Luo in Liquid Crystals Applications and Uses, Vol. 1, World Scientific, Singapore, Chap. 15 (1990).

[60] E.P.Raynes, *Rev.* Phys. Appl., 10, 117 (1975).

[61] N.Wakita, T.Uemura, H.Ohnishi, H.Mizuno and H.Yamazoe Ferroelectrics, 149,229 (1993).

[62] Y.Yamada, N.Yamamoto, K.Mori, K.Nakamura, T.Hagiwara, Y.Suzuki, I.Kawamura, H.Orihara and Y.Ishibashi, Jpn. J. Appl. Phys., 29, 1757 (1990).

[63] M.Yamawaki, Y.Yamada, N.Yamamoto, K.Mori, H.Hayashi, Y.Suzuki, Y.S.Negi, T.Hagiwara, I.Kawamura, H.Orihara and Y.Ishibashi, Proc. 9^{th} *Int* Display Research *Conf.*, Japan Display '89, Kyoto, p. 26 (1989).

[64] M.Johno, A.D.L.Chandani, J.Lee, Y.Ouchi, H.Takezoe, A.Fukuda and K.Itoh, Proc. SID., 31, 129 (1990); (Proc. 9^{th} Int. Display Research Conf., Japan Display '89, Kyoto, p. 22 (1989).

[65] G.H.Brown, Liquid crystals, Vol.2, Part I, Gordon and Breach, New York (1969), Synopsis of Panel Discussion on Applications, pp. 217-232.

[66] E.J.Klein, Astronaut. Aeronaut., 6, 70 (1968).

[67] Sharn Inc. 4801 George Road, Tampa, Florida FL33634 USA (1993). See Designation E 1061-85, Annual book of ASTM standards, 14.01, 866 (1985).

[68] J.T.Crissey, E.Gordy, J.L.Fergason and R.B.Lyman, J. Invest. Dermatol., 43, 89 (1964).

[69] U.Moller and J.Bosjen, Cancer Res., 35, 3116 (1975).

[70] J.Tricoire, *J.Gynecol.* Obstet. Biol. *Reprod.*, 4, 123 (1975).

[71] T.W.Davison, K.L.Ewing, J.L.Fergason, M.Chapman, A.Can and C.C.Voorhis, Cancer., 29, 1123 (1972).

[72] M.Gautherie, J. Phys., **30,** 122 (1969).

[73] M.Gautherie, Y.Quenneville, C.Rempp and C.Gros, J. Radiol., 56, 316 (1975).

[74] H.Kucera and E.Kubista, *Wein. Klin.* Wochenschr., 88, 737 (1976).

[75] V.E.Smirnov and P.M.Lavreshin, *Vestnik Khirugii Imeni II* Grekova., 145, 37 (1990).

[76] C.L.Khetrapal, R.G.Weiss and A.C.Kunwar, in Liquid crystals – Applications and uses, Vol. 2 World Scientific, Singapore, p.225 (1991).

[77] L.Pohl, in Topics in Physical Chemistry, Vol. 3, Liquid Crystals, Springer, New York, p.173 (1994).

[78] R.G.Weiss, Tetrahedron., 44, 3413 (1988).

[79] H.Kelker and R.Hatz, Handbook of Liquid Crystals., Verlag Chemie: Weinheim (1980).

[80] H.Kelker, *Z.* Anal. Chem., 198,254 (1963).

[81] M.J.S.Dewar and J.P.Schroeder, *J.* Am. Chem. *Soc.*, 86,5235 (1964).